of only the direct stimulus effects to the scatter diagram by constructing the cross product of the marginal probability densities (obtained from the two PST histograms). The resulting bivariate density, which contains no diagonal bands, serves as a control. It represents the hypothetical case in which the two neurons fire independently except for shared input caused by the stimulus. Comparison of this control with the observed joint density facilitates the detection of direct interactions and shared input from sources other than the stimulus.

The method described can be extended as follows: When more than two neurons are monitored together with a stimulus train, each spike train can be assigned its own Cartesian coordinate. The resulting $N$-dimensional scatter diagram, although presenting some difficulties in display, can be interpreted in a completely analogous manner to that of the two-dimensional diagrams. For example, a concentration of points about a line parallel to the principal diagonal of the coordinate system corresponds to a set of interactions, or shared input unrelated to the stimulus, involving all of the monitored neurons.

The scatter diagram described here is a supplement to rather than a substitute for the PST and cross-correlation histograms. Weak interactions may be more readily detected in the appropriate histogram. Examination of the histograms can serve as a guide to the detailed interpretation of particular features in the scatter diagram. This combined approach should be particularly applicable, for example, to experiments which seek to associate plasticity of behavior with changes in neuronal interactions.

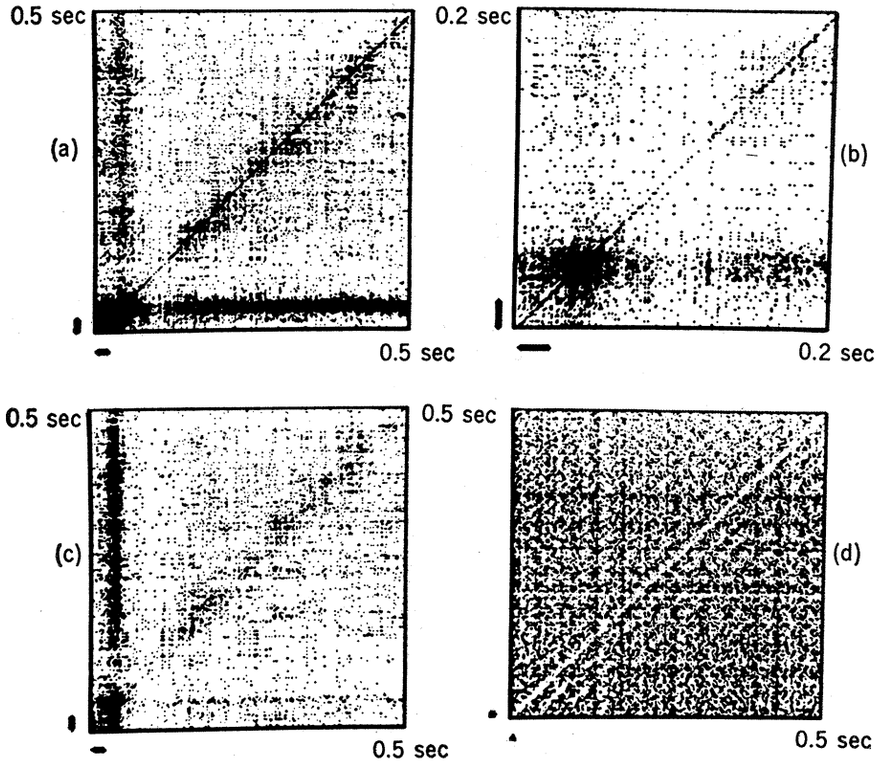


Fig. 2. Joint PST scatter diagrams. Units in auditory cortex of unanesthetized cat. Stimuli were 20-msec noise bursts, two per second, and are indicated by the dark bars. (a) Units 1 and 3: strong vertical and horizontal bands represent the stimulus-caused activity of each unit individually. The different latencies, time courses, and fine structures of the two responses are apparent. The narrow diagonal band represents a direct excitatory interaction between the two neurons with a latency of 3 msec. The wide diagonal band of increased density in central and upper right portion is most plausibly attributed to a weak shared excitatory input. The absence of this wide diagonal band in the lower left portion of scatter diagram indicates inhibition of the inferred common source for some time after the stimulus. (b) Enlargement of lower left portion of (a); differences in vertical and horizontal structure of region of high density and variation of density along the thin diagonal band, presumably reflecting stimulus-related reduction of firing, are shown. (c) Units 2 and 3, same preparation. The wide diagonal band again indicates that the stimulus inhibited shared input from nonstimulus sources. The shared input reaches unit 3 after unit 2, in that the wide diagonal band lies above the principal diagonal. There is no evidence for a direct synaptic connection. (d) Two Purkinje cells in the vermis of anesthetized cat cerebellum during an auditory stimulation by clicks (one click per second). There are no significant vertical or horizontal features, indicating that these units did not respond to the stimulus. Multiple diagonal bands are visible and presumably represent shared input and time delays associated with parallel-fiber input (*2*).


GEORGE L. GERSTEIN
*Departments of Biophysics* and *Physiology, University of Pennsylvania, Philadelphia 19104*

DONALD H. PERKEL
*Department of Mathematics, RAND Corporation, Santa Monica, California 90406*


### References and Notes


1. G. P. Moore, D. H. Perkel, J. P. Segundo, *Ann. Rev. Physiol.* **28**, 493 (1966).
2. D. H. Perkel, G. L. Gerstein, G. P. Moore, *Biophys. J.* **7**, 419 (1967).
3. We propose "peri-stimulus-time" instead of the older restrictive term "post-stimulus-time." The initials PST are thereby preserved.
4. The joint PST density may be defined by the equation

$$\xi_{ab}(t, u) = \lim_{\substack{\Delta t \to 0 \\ \Delta u \to 0}} \frac{1}{\Delta t\, \Delta u} P$$

where $P$ equals probability [spike in A in $(v + t, v + t + \Delta t)$ and spike in B in $(v + u, v + u + \Delta u)$, given the stimulus event at $v$]
5. C. C. Bell and R. J. Grimm, personal communication.


6. Supported by PHS grants NB 05606, NB 07325, FR-15, and by United States Air Force Project RAND.

6 February 1969


## Scanning Electron Microscopy of Cells


Abstract. *The scanning electron energy-analyzing microscope uses characteristic energy losses to provide picture contrast. At different levels of energy loss particular structures are distinguished with high contrast in an unstained section of a cell.*


Electron microscopy of ultrathin sections of biological tissue generally requires electron-opaque staining to obtain suitable contrast for detailed analysis. A heavy atom that selectively attaches to certain cell components (such as nuclei, mitochondria, and lysosomes) is typically used to stain the specimen. The contrast provided by such staining for examination with a conventional electron microscope depends primarily on specimen density. An ideal mechanism for obtaining contrast would be one in which different structures could be shown suc-

cessively in the same section, and which did not require staining with consequent loss of high resolution.

The examination of ultrathin tissue sections without the requirement of staining is possible with a new scanning electron energy-analyzing microscope (*1–4*). This microscope has been designed in such a way as to discriminate atomic or molecular species on the basis of unique energy losses suffered by electrons passing through the material. It differs from the scanning electron microscopes described recently (*5*) in that the distribution of energy in the transmitted electrons provides the information for contrast. In this way cell components with similar densities but different atomic or molecular composition may be distinguished by scanning the same specimen area for different peaks of energy loss; and it is theoretically possible to do this with high resolution. The possibility of doing it was shown in the original description of the microscope (*2*), and the present report demonstrates the possibility of using this approach for the examination of biological material.

A tissue culture method was used to obtain specimens for this study. Monolayers of cells from a strain of a pig kidney cell line were grown in plastic flasks for 72 hours at 37°C. The cells were removed from the surface of the flask with a mixture (1:1) of trypsin-ethylenediaminetetraacetate (0.25 percent), centrifuged, washed several times in warm isotonic balanced-salt solution, fixed 2 hours in glutaraldehyde (2.5 percent), postfixed for 1 hour in osmic acid (1.0 percent), dehydrated through alcohols, and embedded in Epon. Gray and silver sections (500 to 600 Å thick) of the embedded cells were cut and floated onto electron microscope grids for observation with both the Siemens electron microscope and the new scanning electron energy-analyzing microscope. Some sections were stained with uranyl and lead acetate.

Figure 1a is a section of a stained cell photographed with a Siemens electron microscope. Within the cytoplasm the mitochondria appear as dark oblong objects with characteristic internal structure, and the fat bodies are white spheres. The nuclear membrane is obvious and the chromatin material in the nucleus appears as small gray spheres, darker than the substrate of the nucleus. The endoplasmic reticulum in the cytoplasm is about the same shade of gray as the nuclear substrate. Parts (b) and (c) of Fig. 1 are of another cell in an adjacent section from the same material; however, it is unstained and photographed with various energy losses by use of the scanning electron energy-analyzing microscope. As the components within the cell change from white to gray and black, different molecules with comparable densities and atomic composition are brought into contrast. Figure 1b is an unstained cell formed from electrons which have lost no energy ($\Delta E = 0$). The cytoplasm is basically white, and within the matrix are fat bodies (*F*) that appear in most cases to have a gray center with black outer core. The lysosome-like bodies (*L*) are white with no outer dark core, and the mitochondria (*M*) are gray. The endoplasmic reticulum (*ER*) appears white. The chromatin (*C*) within the nucleus is a darker gray than the substrate of the nucleus. The nuclear membrane is slightly distinguishable as two irregular gray circles. Figure 1c is the image formed from electrons that had lost 18 ev of energy ($\Delta E = 18$ ev). The cytoplasm in this photograph is for the most part now gray and most of the fat bodies are now black. They are denser at this energy loss than the other cellular structures. The endoplasmic reticulum has become gray. The lysosome-like bodies are now light gray, and the mitochondria are a lighter gray. The chromatin is rela-

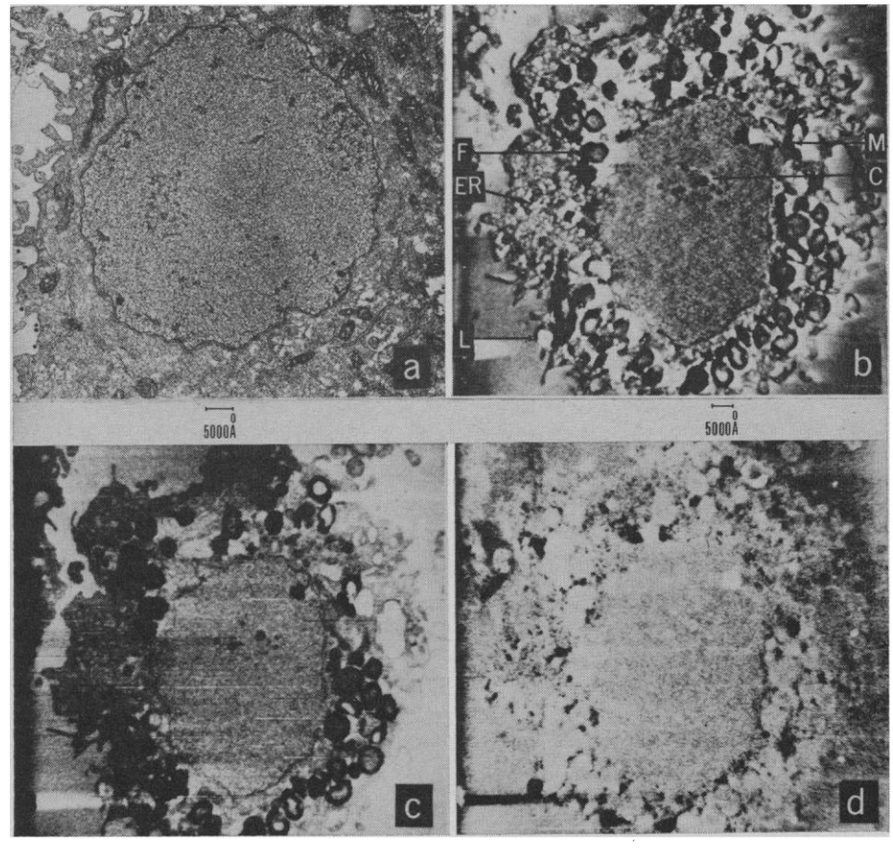


Fig. 1. (a) An electron micrograph (Siemens) of a section (500 to 600 Å thick) of a cell stained with uranyl and lead acetate. (b–d) Scanning electron energy-analyzing micrograph sequences of an unstained cell in the same section as (a), taken with three energy losses, $\Delta E = 0$, 18, and 50 ev. At no energy loss (b) the cytoplasm is essentially white and the fat granules (*F*) have in most cases a gray center with a black outer core. The endoplasmic reticulum (*ER*) appears white. Lysosome-like bodies (*L*) are white, and the mitochondria appear gray. The chromatin (*C*) is a darker gray than the substrate of the nucleus. The nuclear membrane is slightly distinguishable as two irregular gray circles. Changes in density of the different cellular components are brought into contrast at 18 ev (c). The cytoplasm is now gray and the fat bodies are quite dark. The lysosome-like bodies are a pale white and the mitochondria are a lighter gray. The chromatin is relatively unchanged. A more definite change is seen at 50 ev (d). The components in the cell are now either light gray or white. The lysosome-like bodies are now black and the endoplasmic reticulum is dark gray. The nuclear membrane cannot be distinguished, and the matrix in the nucleus is very light.

tively unchanged, but the matrix in the nucleus has become lighter and more uniform, and the nuclear membrane is more sharply defined. With $\Delta E = 50$ ev (Fig. 1d) almost all the components of the cell have changed in contrast and now range from a very light gray to white. Notice that the lysosome-like bodies, and other smaller spheroid bodies, which were white at $\Delta E = 0$, are now black, and the other cellular components are white or gray, indicating that the energy loss spectrum is quite different at this 50-volt peak. The nuclear membrane is no longer distinguishable.

From this preliminary investigation of the cell by electron energy loss, one observes that various ultrastructures can be distinguished in the same cell through changes in image density. The change indicates that there is a substantial amount of information in the transmitted beam of electrons. To obtain this type of information with the conventional electron microscope would require different stains on several consecutive sections. It is hoped that further modification of the microscope, and proper selection of energy levels, may make it possible to localize selectively specific elements, such as metal ions (calcium, iron, magnesium, and others), on the basis of specific energy losses sustained by impinging electrons, and to improve resolution.

AGNES N. STROUD*
LEONARD M. WELTER†
DOROTHY A. RESH, DUANE A. HABECK
A. V. CREWE,‡ J. WALL‡
*Division of Biological and Medical Research, Argonne National Laboratory, Argonne, Illinois,* and *University of Chicago, Chicago, Illinois*

### References and Notes

1. A. V. Crewe, *J. Microscop.* **2**, 369 (1963).
2. ———, *Science* **154**, 729 (1966).
3. A. V. Crewe, D. N. Eggenberger, J. Wall, L. M. Welter, *Rev. Sci. Instr.* **39**, 567 (1968).
4. A. V. Crewe, J. Wall, L. M. Welter, *J. Appl. Phys.* **39**, 5861 (1968).
5. W. E. J. Jaques, J. Coalson, A. Zervins, *Exp. Mol. Pathol.* **4**, 576 (1965); R. F. W. Pease and T. L. Hayes, *Nature* **210**, 1049 (1966); T. L. Hayes, R. F. W. Pease, L. W. McDonald, *Lab. Invest.* **15**, 1320 (1966); R. F. W. Pease, T. C. Hayes, A. S. Camp, N. M. Amer, *Science* **154**, 1185 (1966); R. Christenhuss, Th. Buchner, R. A. Pfeiffer, *Nature* **216**, 379 (1967); P. W. Neurath, M. G. Ampola, H. G. Vetter, *Lancet* **1967-I**, 1366 (1967).
6. Work performed under the auspices of the U.S. Atomic Energy Commission.

* Present address: Pasadena Foundation for Medical Research, Pasadena, Calif.
† Present address: Ultek Division of Perkin-Elmer, Palo Alto, Calif.
‡ Present address: Enrico Fermi Institute, University of Chicago, Chicago, Ill.

10 February 1969

## Actinomycin D: Uptake by Sea Urchin Eggs and Embryos

Abstract. *Actinomycin D is excluded from unfertilized eggs and developing embryos of the sea urchin* Arbacia punctulata *until the blastula hatches. The rate of uptake of actinomycin D by embryos doubles as development progresses after hatching to the gastrula stage.*

Despite the wide use of actinomycin D in investigations of ribonucleic acid and protein synthesis, little is known about the ability of this drug to penetrate intact cells (*1*). This lack of information has resulted in the use of empirical dosage schedules in a variety of widely dissimilar experimental systems. Inhibition of RNA synthesis or protein synthesis after administration of the drug is considered proof of a direct effect of this antimetabolite on genetic transcription. However, the interpretation of experiments in which administration of the drug does not cause inhibition is difficult without evidence that the drug has penetrated to the site of its postulated action.

The marked increase in protein synthesis after fertilization of sea urchin eggs proceeds normally for several hours in the presence of actinomycin D (*2*). Current ideas about the fundamental events of early embryonic development are based, to a large degree, on this observation, particularly the concept that stable maternal messenger RNA's direct the production of early embryonic proteins (*3*).

Because the unfertilized sea urchin egg is almost completely impermeable to polypeptides and amino acids, we investigated the uptake and binding of actinomycin D-$^{14}$C (a polypeptide) in eggs and embryos of the sea urchin *Arbacia punctulata.*

Mature females were induced to spawn into seawater by electroshock (*4*). The eggs were washed in sterile seawater and counted in micropipettes.

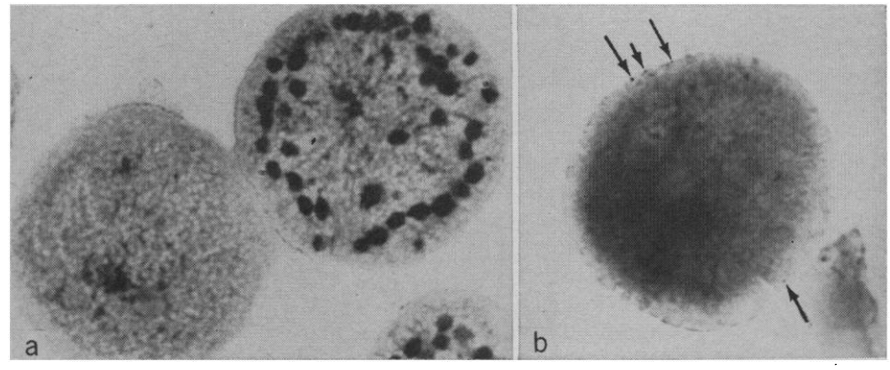


Fig. 1. (a) Control blastula in the upper right hand corner, control unfertilized egg at lower left. No artifactual grains are visible (× 750). (b) Unfertilized egg treated with actinomycin D-$^{14}$C for 4 hours. Grains are visible at periphery (upper left-hand corner), none over the egg itself (× 1013).

Table 1. Radioactivity of unfertilized eggs plus incubation medium compared with that of egg homogenates and incubation medium alone. At time 0, 1 ml of seawater containing 73 $\mu$g of actinomycin D-$^{14}$C (specific activity, 11.4 mc/m$M$) and 127 $\mu$g of unlabeled actinomycin D was added with stirring to a suspension of 460,000 eggs in 9 ml of sterile seawater (final concentration of actinomycin D, 20 $\mu$g/ml). Portions (1 ml) of egg suspension were removed at the times indicated and homogenized directly ("egg-medium homogenate"). The eggs contained in other portions of the suspension were separated from the incubation medium and homogenized in 1 ml of distilled water as described in the text ("egg-water homogenate"). Portions (0.1 ml) of each type of homogenate and of the incubation medium alone were counted in 10 ml of Bray's solution in a liquid scintillation counter. Control cultures without actinomycin D were prepared with each experiment.

| Incubation (min) | "Egg-medium homogenate"* | Radioactivity (count min$^{-1}$ ml$^{-1}$) | |
|---|---|---|---|
| | | Incubation medium | "Egg-water homogenate"* |
| 0 | 101,960 | 102,840 | 980 |
| 10 | | 100,140 | 970 |
| 30 | 103,000 | 110,420 | 774 |
| 60 | 104,000 | 106,410 | 860 |
| 120 | | | 849 |
| 240 | 103,840 | 112,300 | 840 |

* Eggs occupied approximately 1 percent of the volume.